SYNTHESIS, CHARACTERIZATION, AND PROTEIN IMMOBILIZATION STUDY OF PHEMA GRAFTED HYDROXYAPATITE NANOCRYSTALS VIA SURFACE INITIATED RADICAL POLYMERIZATION

L. G. Bach, M. R. Islam, T. B. Mai, T. T. Nga, L. Niranjanmurthi, K. T. Lim*

Department of Imaging System Engineering, Pukyong National University, Busan, 608-737, Korea
** E-mail address: ktlim@pknu.ac.kr*

Keywords: Hydroxyapatite, Poly(2-hydroxyethyl methacrylate), Surface initiated radical polymerization, Protein loading.

Abstract
A bionanocomposite of poly(2-hydroxyethyl methacrylate) (PHEMA) and hydroxyapatite nanocrystals (HAP NCs) was successfully synthesized via surface thiol-lactam initiated radical polymerization (TLIRP) employing grafting from protocol. The surface chemistry, structure, morphology, and size distribution of PHEMA-g-HAP nanocomposites were exclusively investigated by FT-IR, ^{1}H-NMR, GPC, XPS, TGA, XRD, SEM, TEM, and DLS analyses. Covalently formed PHEMA-g-HAP nanocomposites demonstrated an exceptionally good dispersibility in both aqueous and organic solvents. A protein immobilization and release study suggested that the synthesized PHEMA-g-HAP nanocomposites possessed a great affinity towards the Bovine Serum Albumin (BSA) protein.

1 Introduction
Recently, much work has been furnished on the development of new nanocomposites with novel properties for possible applications in drug delivery systems, artificial organs, regenerative medicine, biofunctional materials, bio- and chemosensing, and bioelectronics [1,2]. The use of hydroxyapatite nanocrystals (HAP NCs), $Ca_{10}(PO_4)_6(OH)_2$, has attracted rigorous interest in the construction of artificial bonelike ceramic/polymer composites due to their similarity to the bone minerals in morphology, size, and crystallinity. The HAP NCs not only plays a significant role in maintaining the mechanical properties of the natural bone but also offers a non-toxic and non-immunogenic environment for bioactivity, biocompatibility, solubility, fracture toughness and protein absorption, and can be tailored over for wide range of applications [3,4]. For many applications, the surface functionality is a key factor for controlling the nanoparticle's interaction with biological species, self-assembly dispersion and compatibility with polymeric materials. Poly(2-hydroxyethyl methacrylate) (PHEMA) is widely used as bone cement for fixing total hip prostheses to give suitable mechanical properties to the material. Moreover, its hydrophilicity basically from the hydroxyl groups makes it bio- and blood-compatibility and the end hydroxyl groups of the grafted PHEMA side chains can be converted into various functional derivatives [5].
Several methods have been developed to prepare polymer coatings on inorganic particles such as physical adsorption or chemisorptions. There are mainly two ways to fabricate polymer brushes with covalent bonding by either "grafting to" or "grafting from" approaches [6,7].

The "grafting from" strategy provides high graft density. For this technique, initiating groups should be immobilized on the nanoparticles in first stage. There are several approaches have been developed for functionalization of nanoparticles using "grafting from" strategy, but still are some bottlenecks such as multiple reaction steps or using metal catalyst. Therefore, finding a facile method for grafting polymer on nanoparticles is a crucial interest to the materials scientists. Surface bonded thiol groups are used as chain transfer agents in free radical polymerization because of their high chain transfer constant. The silane coupling reagent, 3-mercaptopropyl-trimethoxysilane (MPTMS), is reportedly used to prepare thiol-terminated silica [8]. Recently, we have found a promising method for grafting polymer from the surface of nanoparticles based on two component initiating system consisting of thiol and butyrolactam (BL) [9-10]. This technique doesn't require many reaction steps to introduce functional groups to the inorganic surface for polymerization with complex structures. Moreover, it does not demand any metal catalyst and the reaction condition is very mild.
Having these instances in hand, a thiol-lactam initiated radical polymerization (TLIRP) strategy was successfully employed to prepare chemically immobilized PHEMA onto HAP NCs. The chemically bonded PHEMA with HAP NCs was investigated by respective physical and spectral techniques. A preliminary study using bovine serum albumin (BSA) as model protein suggested a prospect of PHEMA-*g*-HAP nanocomposites in biomedical applications.

2 Materials and methods

2.1 Materials

2-Hydroxyethyl methacrylate (HEMA) was purified by passing the liquid through a neutral alumina column to remove the inhibitor prior to use. Hydroxyapatite nanocrystals (HAP NCs), (3-mercaptopropyl) trimethoxysilane (MPTMS), butyrolactam (BL), bovine serum albumin (BSA), and phosphate buffered saline (PBS), and all solvents were purchased from Aldrich and used as received.

2.2 Synthesis of HAP NCs having surface thiol groups (HAP-SH)

In a typical process, the HAP NCs (4.0 g) were silanized by MPTMS (1 mL) upon stirring them in a mixed solution of 180 mL of ethanol and 20 mL of water. The mixture was then stirred for 6 h. HAP-SH NCs were purified by several washes with double distilled water. After filtration, the HAP-SH NCs were dried at room temperature to improve the stability of the coating and cured at 100 ^{o}C for 24 h to obtain the final condensed silane on the surface.

2.3 Synthesis of PHEMA-g-HAP nanocomposites via surface TLIRP

0.2 g of HAP-SH, 1.0 g of HEMA, 0.5 g of BL, 2 mL of toluene and a teflon-coated stir bar were placed in a 25 mL round flask equipped with a reflux condenser. The flask was purged with nitrogen, heated to 90 ^{o}C and was kept for stirring. At the end of the reaction, the viscosity increased dramatically. After the desired time, the flask was cooled to room temperature and the reaction mixture was precipitated in diethyl ether. The product was filtered to collect the PHEMA-*g*-HAP nanocomposites and dried in a vacuum oven.

2.4 Protein adsorption and release study of PHEMA-g-HAP nanocomposites

In a typical method, 20 mg of PHEMA-*g*-HAP nanocomposites were immersed in 6 mL of the BSA-dissolved water (200 μg mL^{-1}) under continuous shaking at 37 °C. After 24 h incubation, the slurry was centrifuged, and the amount of remaining protein in the supernatant was measured by bicinchoninic acid assay (BCA) technique. The amount of loaded proteins on the PHEMA-*g*-HAP nanocomposites was calculated by subtracting the value from the initial protein concentration. The protein release from the BSA-loaded PHEMA-*g*-HAP was studied in phosphate buffered saline (PBS, pH = 7), which mimics body fluid. The PHEMA-*g*-HAP nanocomposites with BSA adsorbed on it (20 mg) were immersed in 6 mL of PBS. After the desired time, the slurry was centrifuged, and the amount of protein released from BSA-loaded PHEMA-*g*-HAP nanocomposites in supernatant was measured by UV technique.

2.5 Instrumentation

The changes in the surface chemical bonding of HAP NCs were investigated by Fourier Transformed Infrared Spectra (FT-IR) using a BOMEM Hartman & Braun FT-IR Spectrometer. Surface composition was studied by X-ray Photoelectron Spectroscopy (XPS) (Thermo VG Multilab 2000). Thermogravimetric analysis (TGA) was conducted with Perkin-Elmer Pyris 1 analyzer (USA). Dynamic laser light scattering (DLS) measurements of the nanocomposites was carried out using a Brookhaven laser light scattering instrument. The crystallographic state of modified HAP NCs was determined by a Philips X'pert-MPD system diffractometer (Netherlands). The morphology of the hybrids was captured using Field Emission Scanning Electron Microscopy (FE-SEM, Hitachi JEOL-JSM-6700F, Japan) and Transmission Electron Microscopy (TEM) (Hitachi H-7500 instrument operated at 80 kV). Protein estimation was conducted by a Perkin-Elmer Lambda 40 Ultraviolet–visible Spectrophotometer applying BCA technique.

3 Results and discussion

3.1 Covalent grafting of PHEMA onto HAP NCs

A schematic representation for the chemically synthesis of PHEMA-*g*-HAP nanocomposites using TLIRP technique is illustrated in Scheme 1. At first, MPTMS was reacted with the hydroxyl groups on the surface of HAP NCs *via* ligand-exchanging to covalently introduce thiol groups (HAP-SH). Subsequent grafting polymerization of HEMA from HAP-SH surface was accomplished in the presence of BL to afford PHEMA-*g*-HAP nanocomposites.

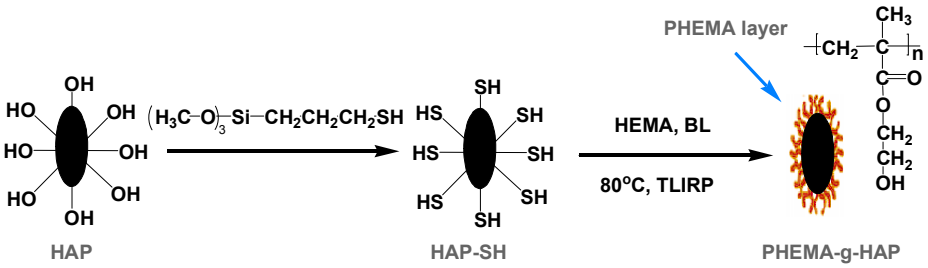

Scheme 1. Synthetic route for the preparation of PHEMA-*g*-HAP nanocomposites using TLIRP technique.

The nature of chemical bond formed through the reaction of MPTMS with surface hydroxyl on HAP NCs and the grafting polymerization of HEMA in the aid of HAP-SH and BL was investigated by FT-IR spectroscopy (Fig. 1). In the FT-IR spectrum of HAP-SH, a new small band in the wavenumber range at 2900-3000 cm^{-1} is observed due to the aliphatic C–H stretching vibration of the CH_3 and CH_2 groups of MPTMS residues as shown in Figure 1B. In addition, the MPTMS functionalized HAP NCs gives a weak but visible absorption band at 2573 cm^{-1} is assigned to the S-H stretching band, which is not observed in the absorption spectrum of HAP NCs, indicating the chemical anchoring of MPTMS onto HAP NCs. FT-IR spectroscopy studies yielded useful qualitative information on the PHEMA-*g*-HAP nanocomposites (Fig. 1C). The broad absorption band at 3022-3647 cm^{-1} is due to O-H stretching. The characteristic bands in the range of 3000-2800 cm^{-1} may be ascribed to the C-H stretching vibrations of the CH_3 and CH_2 groups of PHEMA on the surface of HAP NCs. The PHEMA grafted HAP NCs can be confirmed by a new band appeared at around 1724 cm^{-1} indicates the characteristic carbonyl (C=O) stretching present in PHEMA-*g*-HAP nanocomposites. The absorption bands at 1180-1225 cm^{-1} may arise from the stretching vibrations of -C-O- in the ester groups. All the results indicate that PHEMA chains were chemically immobilized onto the surface of HAP NCs by TLIRP strategy.

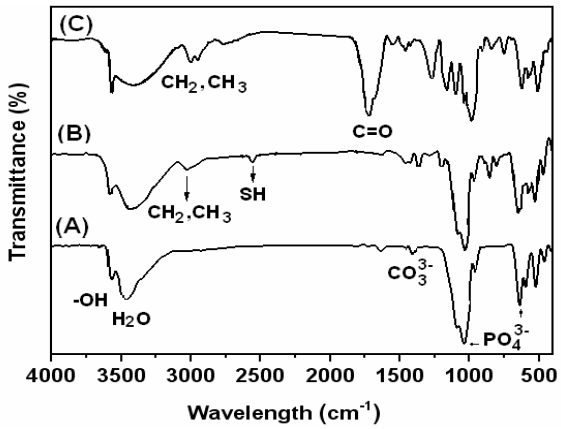

Figure 1. FT-IR spectra of (A) HAP NCs, (B) HAP-SH, and (C) PHEMA-*g*-HAP nanocomposites.

In order to identify the characteristic elements in the HAP NCs, HAP-SH and PHEMA-*g*-HAP nanocomposites, XPS spectra in the binding energy (BE) of 0–700 eV were recorded as shown in Figure 2. The existence of carbon (C1s), oxygen (O1s), phosphorus (P2s, P2p), and calcium (Ca2p) in the HAP NCs surface can clearly be seen in Figure 2A. MPTMS was immobilized on the surface of HAP NCs might offer a condensation reaction to produce a stable initiator monolayer. Figure 2B shows the survey scan of HAP-SH. As expected, significant peaks for carbon at the BE of 284.7 eV, oxygen (532.5 eV), phosphorus (132.9 eV), calcium (351.5 eV), silica (100.9 eV) and sulfur (167.4 eV) are observed. It is noteworthy that in the wide-scan spectrum of HAP-SH, the characteristic S2p peak of the S-H bond confirms the presence of active thiol groups on HAP NCs surfaces which would be susceptible to initiate the subsequent radical polymerization. Upon grafting of PHEMA onto HAP NCs, the XPS scan of PHEMA-*g*-HAP nanocomposites shows that the C1s peak with high intensity slightly shifted to a higher BE, indicating that the polymeric chains were directly grafted from the surfaces of HAP NCs (Fig. 2C).

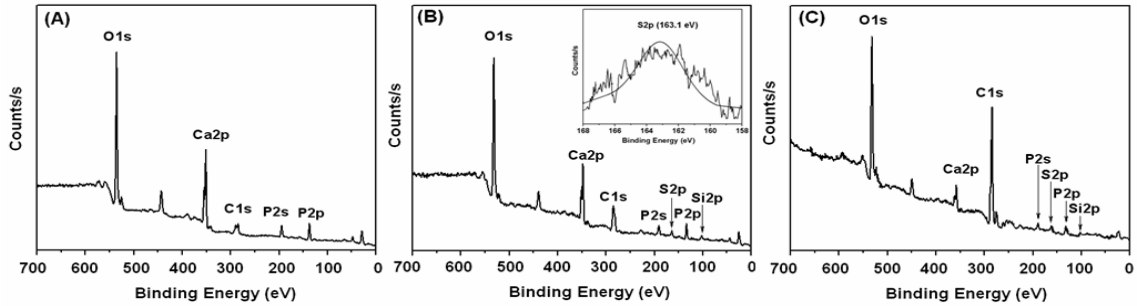

Figure 2. XPS wide-scan spectra of (A) HAP NCs, (B) HAP-SH, and (C) PHEMA-*g*-HAP nanocomposites.

To analyze the chemical structure as well as to determine the number-average molecular weight (M_n) and molecular weight distribution (PDI) of the grafted PHEMA, the PHEMA-*g*-HAP nanocomposites were treated with HCl to cleave PHEMA for HAP NCs surface. ^{1}H-NMR spectrum of cleaved PHEMA is shown in Figure 3A. It is found that the peak at 1.78 ppm (a) is associated with the methylene groups (-C-CH_2-) in the backbone of the PHEMA chain. The peaks at 0.78~1.10 ppm (b) are mainly attributable to the methyl protons of C-CH_3. The peaks at 3.75~3.85 ppm (c) assigned to methylene protons of –C=O-OCH_2 in the HEMA units. The ^{1}H-NMR analysis further suggests that the synthesis of PHEMA-*g*-HAP nanocomposites was successful. By GPC analysis, the M_n and PDI of cleaved PHEMA were found to be 28,700 g/mol and 1.54, respectively.

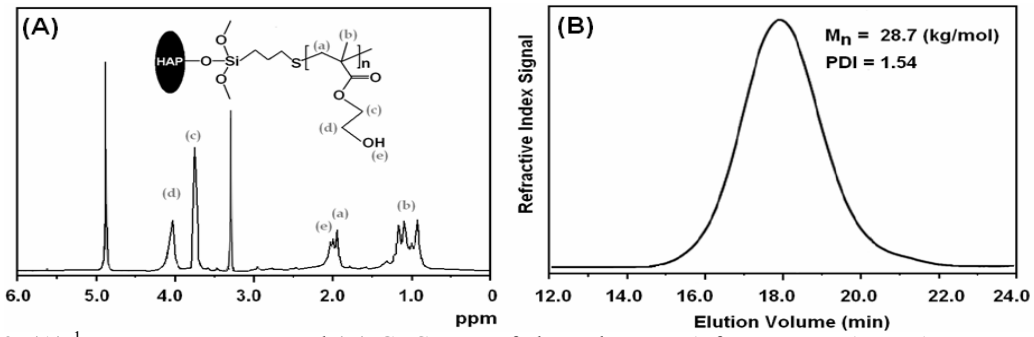

Figure 3. (A) ^{1}H-NMR spectrum, and (B) GPC trace of cleaved PHEMA from PHEMA-*g*-HAP nanocomposites.

To get information regarding thermal stability of the PHEMA-*g*-HAP nanocomposites, TGA analyses of bare and modified HAP NCs were conducted. TGA trace of HAP NCs shows *ca.* 2% of weight loss below 800 °C (Fig. 4A) due to the removal of physically adsorbed water on the surface and the release of the structural water resulted from the bonded hydroxyl groups. In the case of HAP-SH, the weight loss is estimated to be *ca.* 7.2% (Fig. 4B). The as prepared PHEMA-*g*-HAP nanocomposites shows thermal decomposition at temperature range from 285-430 ^{o}C, which is due to the decomposition of grafted PHEMA (Fig. 4C). The degree of PHEMA grafting on the PHEMA-*g*-HAP nanocomposites was measured to be *ca.* 40.1%.

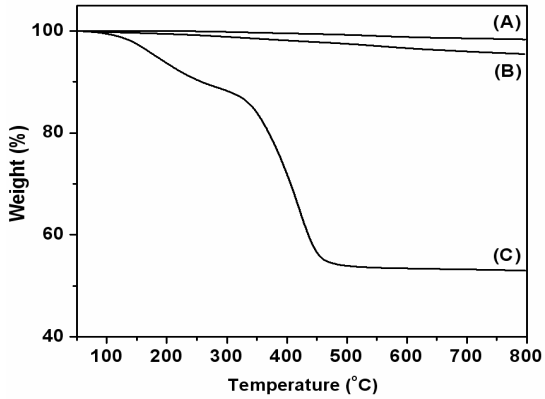

Figure 4. TGA analysis of (A) HAP NCs, (B) HAP-SH, and (C) PHEMA-*g*-HAP nanocomposites.

3.2 Physical structure and morphology of PHEMA-g-HAP nanocomposites

The physical structure and morphology of PHEMA-*g*-HAP nanocomposites were investigated by using XRD, TEM, and SEM analyses. The XRD pattern gave important information of the structure of HAP NCs, HAP-SH and PHEMA-*g*-HAP nanocomposites. The HAP NCs exhibit several sharp peaks at 2θ regions of 26^{o}, 29^{o}, 32–34^{o}, 40^{o}, and 46–54^{o} which are consistent with the crystalline structure of HAP NCs (Fig. 5A). The main diffraction peaks of the (002), (102), (211), (300), (202), (310), (222), (213), and (411) planes from the HAP-SH and PHEMA-*g*-HAP nanocomposites showed that the crystalinity of HAP NCs remained almost unchanged (Fig. 5B-C). Moreover, any secondary phases were not formed due to the chemical reaction and the maintenance of crystalline phase of HAP NCs. The results indicate that the covalent grafting of PHEMA did not alter the physical structure of HAP NCs.

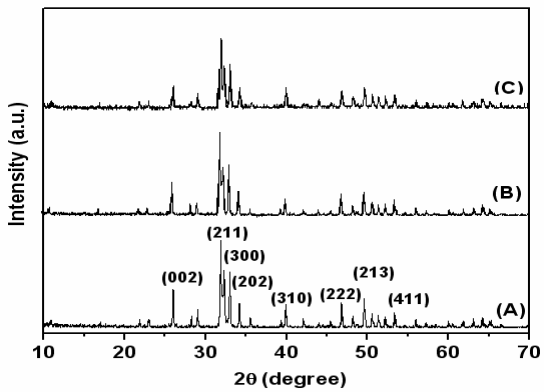

Figure 5. X-ray diffraction patterns of (A) HAP NCs, (B) HAP-SH, and (C) PHEMA-*g*-HAP nanocomposites.

FE-SEM and TEM were employed to analyze directly the morphology of HAP NCs, and PHEMA-*g*-HAP nanocomposites. The HAP NCs are seen as agglomerates with irregular shape and size as shown in the FE-SEM image (Fig. 6A). Upon grafting of PHEMA onto the surface of HAP NCs, the apparent size and shape of NCs were changed which can be easily observe by taking a close look onto the FE-SEM image of modified structure (Fig. 6B). The irregular NCs of HAP are observed to be encapsulated by soft polymer layer. From TEM images, it can be seen that the HAP NCs are acicular crystals and aggregated into micro-scale clusters. The crystallinity of PHEMA-*g*-HAP nanocomposites is observed to be resembled with that of HAP NCs which is good agreement with XRD results. In TEM images, the HAP NCs are visible as dark contrast areas and seen uniformly dispersed throughout the polymer matrices, while the light PHEMA shell formed fringes surrounding HAP NCs cores (Fig. 6D).

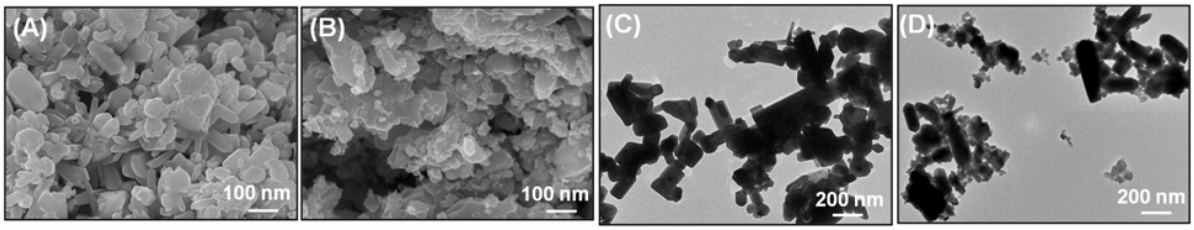

Figure 6. FE-SEM images (A, B) and TEM images (C, D) of HAP NCs (A,C) and PHEMA-*g*-HAP nanocomposites (B, D).

As HAP NCs usually form large micro-scale aggregates in solvent, so the colloidal stability of the HAP NCs in solutions is another challenging aspect for fabrication of the HAP NCs in polymer matrix. The HAP NCs and PHEMA-*g*-HAP nanocomposites were dispersed in distilled methanol followed by ultrasonication for 15 min as shown in Figure 7. The PHEMA grafted HAP NCs exhibited excellent colloidal stability and maintained a stable dispersion up to monitoring period of 12 h. However, the dispersion made from the un-grafted HAP NCs did not maintain colloidal stability and completely precipitated out within a few minutes (Fig. 7B). The improved dispersion of PHEMA-*g*-HAP nanocomposites may be happened due to reduction of surface energy of HAP NCs because of PHEMA immobilization. In order to get idea on the particles size distribution of HAP NCs and PHEMA-*g*-HAP nanocomposites, hydrodynamic diameters of these nanoparticles were measured by DLS. In the case of HAP NCs, the mean hydrodynamic diameter of aggregated particles is *ca.* 172 nm (Fig. 7E). Nanometer scale size resulted in high surface energy so much aggregation of HAP NCs in aqueous system was occurred, so the mean size reflects the aggregation of several HAP NCs. On the other hand, Figure 7F shows the size distribution of homogeneous nanocomposites of PHEMA-*g*-HAP, which reflects a narrow size distribution of *ca.* 70 nm. All above results illustrate that PHEMA have a significant role in the dispersion of HAP NCs in solvents.

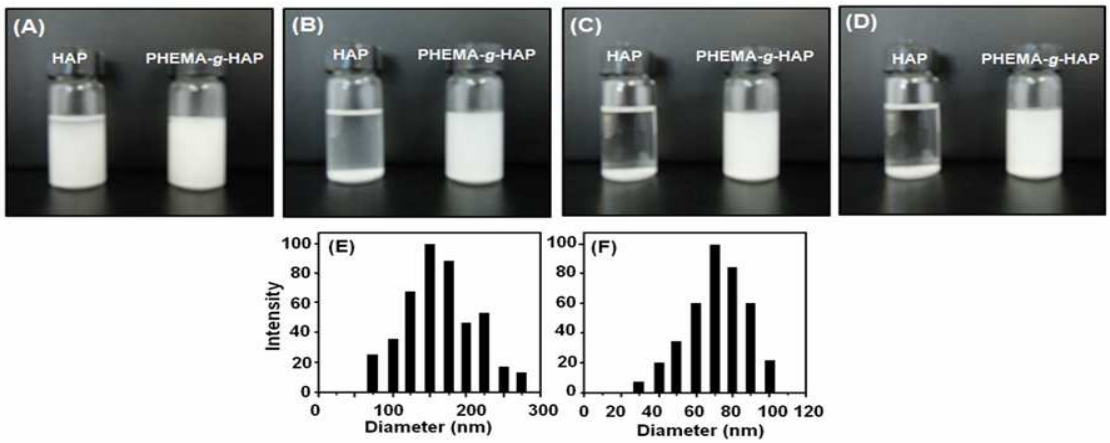

Figure 7. The colloidal stability of HAP NCs and PHEMA-*g*-HAP dispersion in methanol after (A) 0 min, (B) 5 min, (C) 2 h and (D) 12 h, and particle size distribution of (E) HAP NCs, (F) PHEMA-*g*-HAP nanocomposites.

3.3 Adsorption and desorption of proteins on PHEMA-g-HAP nanocomposites

Modification of HAP NCs by PHEMA may enable them molecule-loading capacity with better controlled since PHEMA has the hydroxyl groups in its structure. In order to achieve effective protein release, well regulation of the adsorbed and desorption of protein on PHEMA-*g*-HAP nanocomposites is important. To evaluate the phenomena, the adsorption behavior of BSA on HAP NCs and PHEMA-*g*-HAP nanocomposites was investigated in the protein solution at various concentrations. The result showed that the adsorbed amount of BSA on PHEMA-*g*-HAP nanocomposites increased linearly from 0–200 mg/mL in the protein solution and remained almost constant beyond 200 mg/mL (Fig. 8). The adsorbed amount of BSA on HAP NCs showed a typical Langmuir's isotherm. This fact suggests that BSA molecules efficiently adsorbed on the PHEMA-*g*-HAP nanocomposites. Generally, carriers for the drug delivery need the capacity to regulate the release of drugs as well as their loading. To understand the release behavior of BSA loaded PHEMA-*g*-HAP nanocomposites, the BCA assay was conducted to estimate the released BSA in PBS media. When PHEMA-*g*-HAP/BSA was immersed in PBS at pH 7.0, the quantity of released BSA gradually increased with time and reached following a plateau state. It was observed that the BSA release profile from PHEMA-*g*-HAP nanocomposites was in controlled manner i.e. 75% of BSA released in 16 days.

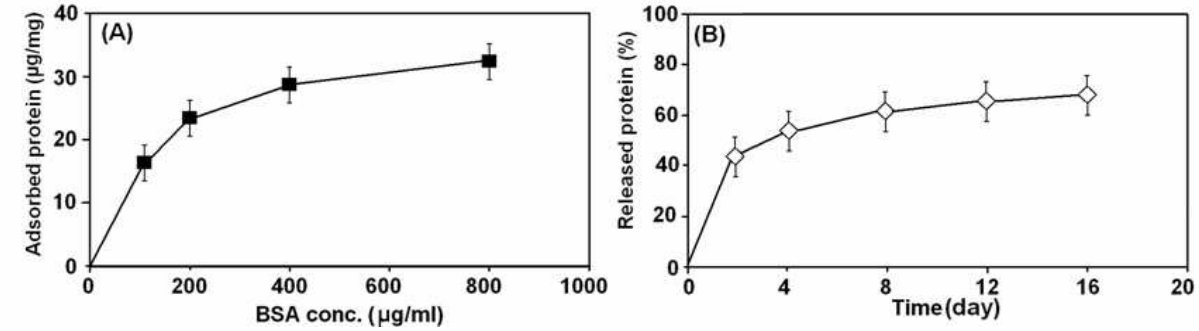

Figure 8. (A) The chart of the BSA adsorption on PHEMA-*g*-HAP nanocomposites, and (B) the release of BSA from BSA-loaded PHEMA-*g*-HAP nanocomposites.

3 Conclusions

Biocompatible PHEMA was grafted onto HAP NCs to afford PHEMA-*g*-HAP nanocomposites by surface thiol-lactam initiated radical polymerization using *grafting from* approach. The chemical modification of biodegradable HAP NCs by PHEMA was

investigated by FT-IR, ^{1}H NMR, GPC and XPS. The data suggested that PHEMA was covalently attached with HAP NCs. The phase compositions and the surface morphology of the synthesized PHEMA-*g*-HAP nanocomposites were studied using XRD, FE-SEM, and TEM. It was found that the HAP NCs were well dispersed in the PMMA matrix without altering its original crystallinity. TGA scan of the nanocomposites revealed that the amount of PHEMA onto HAP NCs surface reached at *ca.* 40.1%. The PHEMA-*g*-HAP nanocomposites showed excellent dispersibility in solvents. The PHEMA-*g*-HAP nanocomposites offered a controlled BSA protein delivery system.

Acknowledgments
This work was supported by the Korea Science and Engineering Foundation (KOSEF) grant funded by the Korea government (MEST) (No. R01-2008-000-21056-0) and the second stage of the BK21 program.

References

[1] Singh M.K., Shokuhfar T., Gracio J.J.A., Sousa A.C.M., Fereira J.M.D.F., Garmestani H., Ahzi S. Hydroxyapatite modified with carbon-nanotube-reinforced poly(methyl methacrylate): A nanocomposite material for biomedical applications. *Adv. Funct. Mater.*, **18**, 694–700 (2008).
[2] Matsumoto T., Okazaki M., Inoue M., Yamaguchi S., Kusunose T., Toyonaga T., Hamada Y., Takahashi J. Hydroxyapatiteparticles as acontrolledreleasecarrier of protein. *Biomaterials*, **25**, 3807–3812 (2004).
[3] Yamada Y., Kurumada K., Susa K., Umeda N., Pan G. Method of fabrication of submicron composite microparticles of hydroxyapatite and ferromagnetic nanoparticles for a protein drug carrier. *Adv. Powder Technol.*, **18**, 251-260 (2007).
[4] Venkatesan P., Puvvada N., Dash R., Kumar B.N.P., Sarkar D., Azab B., Pathak A., Kundu S.C., Fishe P.B., Mandal M. The potential of celecoxib-loaded hydroxyapatite-chitosan nanocomposite for thetreatment of colon cancer. *Biomaterials*, **32**, 3794-3806 (2011).
[5] Weaver J.V.M., Bannister I., Robinson K.L., Bories-Azeau X., Armes S.P. Stimulus-responsive water-soluble polymers based on 2-hydroxyethyl methacrylate. *Macromolecules*, **37**, 2395-2403 (2004).
[6] Wang Y., Dai J., Zhang Q., Xiao Y., Lang M. Improved mechanical properties of hydroxyapatite/poly(ε-caprolactone)scaffolds by surface modification of hydroxyapatite. *Appl. Sur. Sci.*, **256**, 6107-6112 (2010).
[7] Wei J., He P., Liu A., Chen X., Wang X., Jing X. Surface modification of hydroxyapatite nanoparticles with thermal-responsive PNIPAM by ATRP. *Macromol. Biosci.*, **9**, 1237-1246 (2009).
[8] Zhou F., Liu W., Chen M., Sun D.C. A novel way to prepare ultra-thin polymer films through surface radical chain-transfer reaction. *Chem. Commun.*, **23**, 2446-2447 (2001).
[9] Hwang H.S., Bae J.H., Kim H.G., Lim K.T. Synthesis of silica–polystyrene core–shell nanoparticles *via* surface thiol-lactam initiated radical polymerization. *Eur. Polym. J.* **46**, 1654-1659 (2010).
[10] Bach L.G., Islam M.R., Kim J.T., Seo S.Y., Lim K.T. Encapsulation of Fe_3O_4 magnetic nanoparticles with poly(methyl methacrylate) via surface functionalized thiol-lactam initiated radical polymerization. *Appl. Sur. Sci.*, **258**, 2959-2966 (2012).